

# UNIMO-3: Multi-granularity Interaction for Vision-Language Representation Learning

**Hao Yang**

Harbin Institute of Technology  
hyang@ir.hit.edu.cn

**Can Gao**

Baidu Inc., Beijing, China  
gaocan01@baidu.com

**Liu Hao**

Baidu Inc., Beijing, China  
liuhao24@baidu.com

**Xinyan Xiao**

Baidu Inc., Beijing, China  
xiaoxinyan@baidu.com

**Yanyan Zhao**

Harbin Institute of Technology  
yyzhao@ir.hit.edu.cn

**Bing Qin**

Harbin Institute of Technology  
qinb@ir.hit.edu.cn

## Abstract

Vision-and-language (VL) pre-training, which aims to learn a general representation of image-text pairs that can be transferred to various vision-and-language tasks. Compared with modeling uni-modal data, the main challenge of the VL model is: how to learn the cross-modal interaction from multimodal data, especially the fine-grained interaction. Existing works have shown that fully transformer-based models that adopt attention mechanisms to learn in-layer cross-model interaction can demonstrate impressive performance on various cross-modal downstream tasks. However, they ignored that the semantic information of the different modalities at the same layer was not uniform, which leads to the cross-modal interaction collapsing into a limited multi-modal semantic information interaction. In this work, we propose the UNIMO-3 model, which has the capacity to simultaneously learn the multi-modal in-layer interaction and cross-layer interaction. UNIMO-3 model can establish effective connections between different layers in a cross-modal encoder, and adaptively capture the interaction between two modalities at different levels. The experimental results show that our model achieves state-of-the-art performance in various downstream tasks, and through ablation study can prove that effective cross-layer learning improves the model’s ability of multimodal representation.

## 1 Introduction

Vision-and-language pre-training (VLP) aims to use large-scale image-text pair data to learn and simulate the human ability to understand the world through vision and language. VLP has been proven can achieve excellent performances on various VL downstream tasks, such as visual question answering (VQA) (Antol et al., 2015; Goyal et al., 2017), visual entailment(Xie et al., 2019) and image-text retrieval(Lin et al., 2014; Plummer et al., 2015). Meanwhile, VLP can also benefit a series of uni-

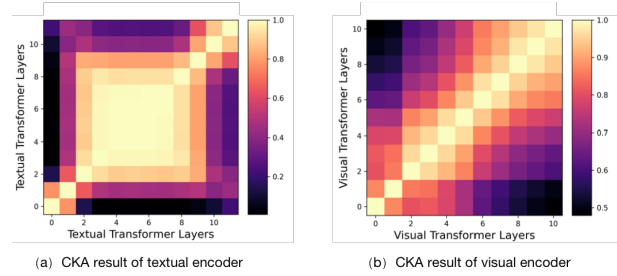


Figure 1: Centered kernel alignment (CKA) results of METER(Dou et al., 2022) uni-modal encoders.

modal tasks(Wang et al., 2018; Krizhevsky et al., 2009) without training a new model from scratch.

In other words, VLP aims to learn a shared embedding space for both text and images, the paired image-text samples are close to each other, while unpaired samples are separated from each other. It is relatively easy to learn such a shared embedding space for text-image matching, such as text-image retrieval task. Previous works (Radford et al., 2021; Jia et al., 2021) have achieved impressive results using image-text matching (ITM) pre-training task and contrastive learning techniques. However, for more complex tasks such as visual question answering (VQA), the VLP model needs to pay more attention to the fine-grained information in image-text pairs. How to improve the ability of the model to perceive, interact and fuse multimodal information with different granularity is crucial for the further development of the VLP model.

Previous works (Li et al., 2020; Tan and Bansal, 2019; Chen et al., 2020; Huang et al., 2020; Zhang et al., 2021) often rely on the object detection models to extract image features or encode the entire image, which dependent on external visual models (such as Fast(er) R-CNN (Ren et al., 2015)). Zeng et al. (2021) proposed an explicit learning multi-granularity vision-language alignment method XVLM, but this method relies on the fine-grained annotation information in the data to

establish fine-grained supervision. With the introduction of Vision Transformers (Dosovitskiy et al., 2020), the model using ViT as the visual encoder and combining with the Two-tower structure has achieved impressive performance in downstream tasks. These models (Dou et al., 2022; Wang et al., 2021) typically leverages the output of the final layer of the uni-modal encoder as input to the cross-modal encoder, the vision and language modalities can be jointly modeled by transformers. The output features of each layer of the uni-modal encoder exhibit noticeable differences in terms of information granularity. For instance, the output of lower layer text encoder contains word-level information, whereas the output of higher layer conveys global semantic information. Similar discrepancies can be observed in the image encoder. Therefore, these methods neglect to enhance the interaction modeling of multimodal information at different semantic granularity.

Xu et al. (2022) proposes to enhance the cross-modal alignment and fusion of uni-modal features at different semantic levels from bottom to top by establishing the bridge layer between the top layers of uni-modal encoders and the cross-modal encoder. We found that the output features from different layers in the end-to-end transformer-based model contain semantic information of different granularity. As shown in Figure 1, we adopt centered kernel alignment (CKA) to visualize the output layer features similarity of uni-modal encoder. Centered kernel alignment is a representation similarity metric that computes features normalized similarity in terms of the Hilbert-Schmidt Independence Criterion (HSIC). However, due to the modal differences, we found that the single link at the same layer of uni-modal encoder and multi-modal encoder is relatively limited. We propose the UNIMO-3 model which establishes effective links between the fusion encoder layer with all the uni-modal encoder layers, enabling the model to better leverage the multi-layer features of the uni-modal encoder and adaptively capture interactions between multimodal information at different granularities.

In our extensive set of experiments, we show that our method achieves competitive performance compare with the VLP models that with same pre-training data and a similar number of parameters. Specifically, with only 4M images for pre-training, UNIMO-3 achieves a new SOTA of 78.88% on

the VQAv2 test-std set. UNIMO-3 also outperform other baseline models when further scaling the model, achieves 81.27% on the VQAv2 test-std set. This result outperforms even the models with more pre-training data and larger number of paramters.

Our main contributions are as follows: (1) We found that the existing VLP models lack to learn the cross-modal interaction in different granularity. (2) We introduce a new model structure, the UNIMO-3 model, which utilizes a fusion encoder that adaptively selects multi-layer output features from uni-modal encoders using the gating mechanism to enable multi-granularity interaction of multimodal information. (3) Through a series of experiments, UNIMO-3 achieves state-of-the-art results and outperforms other models on a range of downstream validation datasets.

## 2 Related Work

### 2.1 Vision-Language Pre-training Models

The VLP model aims to learn a shared embedding space for both text and images by utilizing large-scale image-text pair datasets that are collected from the public web. Paired images and texts are positioned in close proximity within the feature space, while unpaired samples are separated from each other. VLP model has been proven to perform well in downstream visual tasks, language tasks and multimodal tasks. Some early VLP models followed a pipeline approach and utilized external models as visual encoder such as Faster R-CNN and ResNet to extract visual features. Since the emergence of Vision Transformer, some work has made better performance in downstream tasks by using ViT as a visual encoder and combining with the two-tower model structure. These models generally take the output feature of uni-modal encoder’s last layer as the input of cross-modal fusion encoder, and rely on the cross-modal learning mechanism (such as dot product, co-attention mechanism) in the fusion encoder to learn the shared embedding space for both text and images.

Dou et al. (2022) compared the effects of these models on different structural designs and the selection of pre-training tasks through rich experiments, and selected the optimal combination to achieve the state-of-the-art effect in multiple downstream tasks, as illustrated in Figure 2 (a). Xu et al. (2022) proposed to enhance the interaction of cross-modal information at different semantic levels by using

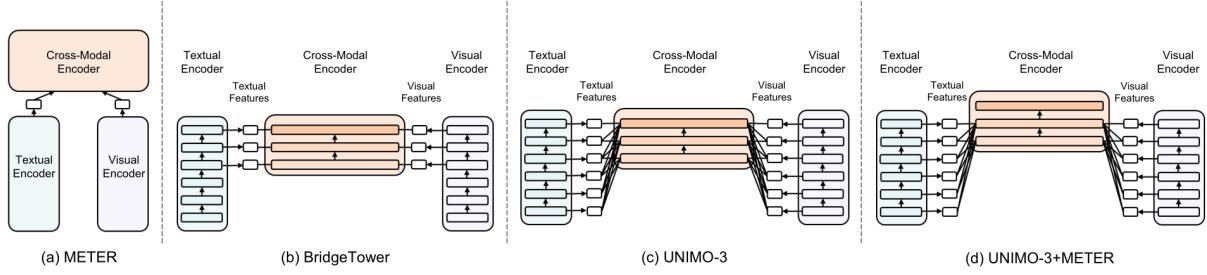


Figure 2: TWO-TOWER vision-language models: (a) METER(Dou et al., 2022) model structure. (b) BridgeTower(Xu et al., 2022) structure, establish connections between top layers of the uni-modal encoder and the cross-modal encoder layers. (c) UNIMO-3 structure, cross-layer multi-granularity interaction. (d) UNIMO-3 and METER structure, establish cross-layer interactive links only at the bottom layer, keeping the number of cross-modal encoder layers unchanged.

the bridge layer to establish connections between top layers of the uni-modal encoder and the cross-modal encoder layers, which resulted in improved performance, as illustrated in Figure 2 (b). As shown in Figure 2 (c) and (d), we draw inspiration from the multi-layer feature utilization, we believe that the establishment of cross-layer connection rather than the interaction of the same layer can bring multi-granularity interaction of multi-modal information and achieve fine-grained cross-modal fusion.

### 3 Approach

#### 3.1 Visual Encoder

Since the CLIP’s visual encoder has been proven beneficial for downstream VL tasks in previous works (Xu et al., 2022; Dou et al., 2022; Shen et al., 2021), we adopt CLIP-ViT-B/16 as the pre-trained visual encoder. Given the input image  $I \in \mathbb{R}^{3 \times H \times W}$  where 3,  $H$  and  $W$  represent the number of channels, height and width of the image, the ViT split the image into  $N$ -patch sequence,  $N = \frac{H \times W}{p^2}$  where  $(P, P)$  is the image patch resolution and a patch  $p \in \mathbb{R}^{3 \times p^2}$ . The input visual representation:

$$V_0 = [E_{[class]}; p_1 W_1^p; \dots; p_N W_N^p] + V^{pos}, \quad (1)$$

where  $V_0 \in \mathbb{R}^{D_v \times (N+1)}$ ,  $E_{[class]}$  represent the prepended token to the patch sequence,  $W^p \in \mathbb{R}^{D_v \times (3 \times p^2)}$  is the trainable linear projection layer,  $V^{pos} \in \mathbb{R}^{D_v \times (N+1)}$  is learnable position embeddings,  $D_v$  is the dimension of the visual encoder. The visual representation in the  $l$ -th layer visual encoder:

$$V_l = Encoder_l^V(V_{l-1}), l = 1, \dots, L_V, \quad (2)$$

where  $L_V$  is the number of visual encoder layers.

#### 3.2 Textual Encoder

Similar to previous work, we adopt RoBERTa-base as our textual encoder. Given the  $M$ -word input sentence  $S = (w_1, w_2, \dots, w_M)$ , we first add " $[\langle s \rangle]$ " token and " $[\langle /s \rangle]$ " token at the sequence  $S$  start position and end position, and then tokenize the obtained new sequence. The input textual representation:

$$T_0 = [E_{[\langle s \rangle]}; E_{w_1}; \dots; E_{w_M}; E_{[\langle /s \rangle]}] + T^{pos}, \quad (3)$$

where  $T_0 \in \mathbb{R}^{D_t \times (M+2)}$  is the word embedding matrix,  $M$  is the number of tokens,  $D_t$  is the dimension of the textual encoder, and  $T^{pos}$  is the positional embeddings matrix. The textual representation in the  $l$ -th layer textual encoder:

$$T_l = Encoder_l^T(T_{l-1}), l = 1, \dots, L_T, \quad (4)$$

where  $L_T$  is the number of textual encoder layers.

#### 3.3 Cross-modal Encoder

The fusion encoder plays a crucial role in the VLP model as it facilitates cross-modal interactive learning. Previous research has demonstrated that the transformer structure, which incorporates cross-attention mechanism and self-attention mechanism, yields optimal performance for cross-modal interactive learning in the fusion encoder. Our UNIMO-3 model is based on a similar structure, with each fusion encoder layer consisting of a visual and text component. These components comprise a multi-headed self-attention (MSA) block, a multi-headed cross-modal attention (MCA) block, and an FFN block.

$$Z_l^T, Z_l^V = Encoder_l^F(\tilde{Z}_{l-1}^T, \tilde{Z}_{l-1}^V), l = 1, \dots, L_F \quad (5)$$

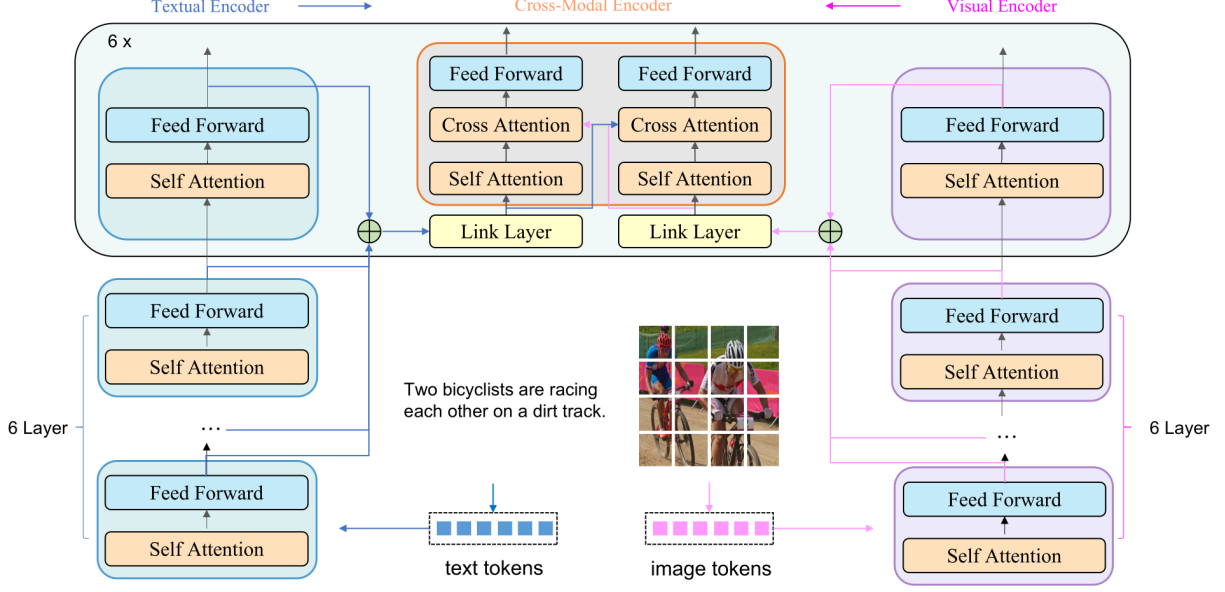


Figure 3: The overview of UNIMO-3 model architecture.

where  $Z_l^T, Z_l^V \in \mathbb{R}^{D_f}$  represent the output features of the  $l$ -th fusion encoder layer, and  $\tilde{Z}_{l-1}^T, \tilde{Z}_{l-1}^V \in \mathbb{R}^{D_f}$  represent the input of the  $l$ -th fusion encoder layer.  $L_F$  is the number of fusion encoder layers.

Our proposed UNIMO-3 model utilizes a gate-based cross-layer feature selection method. The input features of the fusion encoder are derived from multi-layer output features of the uni-modal encoder rather than solely from the last layer.  $Z_0^T$  and  $Z_0^V$  are initialized with the last-layer representations from pre-trained uni-modal encoders before the start interaction layer  $S$ :

$$Z_0^T = W^T T_{L_{S-1}} + T^{type}, \quad (6)$$

$$Z_0^V = W^V V_{L_{S-1}} + V^{type}, \quad (7)$$

where  $W^T \in \mathbb{R}^{D_f \times D_t}$ ,  $W^V \in \mathbb{R}^{D_f \times D_v}$ ,  $T^{type}$ ,  $V^{type}$  are learnable parameters.

In each layer  $l$  of the fusion encoder in UNIMO-3, the input involves interactions between the output of the previous layer  $l-1$  and the output features of the uni-modal encoder across multiple layers, which is different from BridgeTower (Xu et al., 2022) that only considering a single layer. We utilized gating mechanisms for selecting and filtering uni-modal feature across layers, which allows interactions between uni-modal information of different granularities in cross-modal interactions. Each textual parts in fusion encoder layers are connect with

textual encoder layers:

$$g_t = \text{Sigmoid}(W^{G_T} T_{L_t} + b_T + Z_{l-1}^T), \quad (8)$$

$$\tilde{Z}_{l-1}^T = \text{LayerNorm}\left(\sum_{L_t}^{l-1} Z_{l-1}^T + g_t T_{L_t}\right), \quad (9)$$

where  $g_t$  represent the gate value,  $L_t = 1, \dots, l-1$  is the textual encoder layer,  $W^{G_T}, b_T$  are learnable parameters. We adopt sigmoid function to calculate the gate value of the textual feature  $T_{L_t}$  and link with the cross-modal layer base on the gate value. We follow BridgeTower to use (Add&Norm) as the link layer. It is similar for visual parts:

$$g_v = \text{Sigmoid}(W^{G_V} V_{L_v} + b_V + Z_{l-1}^V), \quad (10)$$

$$\tilde{Z}_{l-1}^V = \text{LayerNorm}\left(\sum_{L_v}^{l-1} Z_{l-1}^V + g_v V_{L_v}\right), \quad (11)$$

This structural-level enhancement improves the model's ability to handle fine-grained multi-modal information.

### 3.4 Pre-training Tasks

As observed in the ablation experiments of METTER (Dou et al., 2022), in contrast to that the masked image modeling tasks lead to performance improvement in the pre-training of the region-based VLP models, the masked image modeling tasks resulted in a decrease in performance for transformer-based VLP model. Meanwhile, they found that the

Model	#Pre-train Images	Visual backbone	Test-Dev		Test-Standard		Overall
			Overall	Yes/No	Number	Other	
Base-Size models							
ViLT-base	4M	ViT-B-384/32	71.26	-	-	-	-
UNITER	4M	Faster R-CNN	72.70	-	-	-	72.91
VILLA	4M	Faster R-CNN	73.59	-	-	-	73.67
UNIMO-2-base	4M	ViT-B/16	76.31	-	-	-	76.42
ALBEF-base*	14M	DeiT-B-224/16	75.84	-	-	-	76.04
UNIMO-2-base	4M	ViT-B/16	76.31	-	-	-	76.42
METER-CLIP-ViT-base	4M	CLIP-ViT-B-224/16	77.68	92.49	58.07	69.2	77.64
OFA-base*	54M	ResNet-101	77.98	-	-	-	78.07
SimVLM-base	1.8B	ResNet-101	77.87	-	-	-	78.14
BLIP-base*	129M	DeiT-B-224/16	78.24	-	-	-	78.17
Bridge-Tower-base	4M	CLIP-ViT-B-224/16	78.66	92.92	<b>60.69</b>	70.51	78.73
UNIMO-3-base	4M	CLIP-ViT-B-224/16	<b>78.75</b>	<b>93.20</b>	60.65	<b>70.60</b>	<b>78.88</b>
Large-Size Models							
UNITER-Large	4M	Faster R-CNN	73.82	-	-	-	74.02
VILLA-Large	4M	Faster R-CNN	74.69	-	-	-	74.87
UNIMO-Large	4M	Faster R-CNN	75.06	-	-	-	75.27
VinVL-Large	5.7M	ResNeXt-152	76.52	92.04	61.50	66.68	76.63
SimVLM-Large	1.8B	ResNet-152	79.32	-	-	-	79.56
VLMo-Large	4M	BEiT-L-224/16	79.94	-	-	-	79.98
OFA-Large	54M	ResNet-152	80.43	93.32	<b>67.31</b>	72.71	80.67
BridgeTower-Large	4M	CLIP-ViT-B-224/14	81.25	94.69	64.58	<b>73.16</b>	81.15
UNIMO-3-large	4M	CLIP-ViT-B-224/14	<b>81.26</b>	<b>94.86</b>	65.12	73.02	<b>81.27</b>
Huge or even Larger Size Models							
METER-HUGE	14M	Florence-CoSwin-H	80.33	94.25	64.37	72.30	80.54
OFA-HUGE	54M	ResNet-152	82.00	94.66	71.44	73.35	81.98
Flamingo	2.3B	NFNet-F6	82.00	-	-	-	82.10
CoCa	4.8B	ViT-G-288/18	82.30	94.55	70.25	74.46	82.33
BEiT-3	28M	BEiT-3	84.19	96.43	73.63	75.92	84.18
PaLI	1.6B	ViT-E-224	84.30	96.13	69.07	77.58	84.34

Table 1: Comparisons with previous models on visual question answering (VQAv2). The best score is bolded. The models are divided into base size and large/huge size. B, N and M in ViT-B-N/M denote the model size, image resolution and patch size, respectively. \* indicates that the model also uses VG-QA data to fine-tune on VQAv2. ★ denotes the model is trained from scratch. “# Pre-train Images” denotes the number of images in VLP (the images for pre-trained visual and textual backbones are not counted).

Model	SNLI-VE		Flickr30k						
	dev	test	IR@1	IR@5	IR@10	TR@1	TR@5	TR@10	RSUM
Pre-trained with >4M images									
ALIGN(1.8B)	-	-	84.90	97.40	98.60	95.30	99.80	100.0	576.0
ALBEF(14M)	80.80	80.91	85.60	97.50	98.90	95.90	99.80	100.0	577.7
Pre-trained with =4M images									
UNIMO	80.10	79.10	74.66	93.40	-	89.70	98.40	-	-
UNIMO-2	<b>81.97</b>	<b>81.48</b>	80.14	95.58	-	92.01	99.31	-	-
UNITER-Large	79.39	79.38	75.60	94.10	96.80	87.30	98.0	99.20	550.9
UNIMO-Large	81.11	80.63	78.00	94.20	97.10	89.40	98.80	99.80	557.5
ALBEF	80.14	80.30	82.80	96.70	98.40	94.30	99.40	99.80	571.4
METER-CLIP-ViT	80.86	81.19	82.20	96.30	98.40	94.30	99.60	99.90	570.7
Bridge-Tower	81.11	81.19	<b>85.80</b>	<b>97.60</b>	98.90	94.70	99.61	<b>100.00</b>	<b>576.6</b>
UNIMO-3	81.29	81.23	84.94	97.44	<b>99.00</b>	<b>95.40</b>	<b>99.70</b>	99.90	576.4

Table 2: Comparisons with models pre-trained with 4M images on visual entailment, and image retrieval (IR) and text retrieval (TR) tasks.

masked language modeling (MLM) task and image-text matching (ITM) task can bring performance improvements on downstream tasks. Therefore, we pre-train our UNIMO-3 model with MLM task and ITM task.

**Masked Language Modeling.** Masked Language Modeling (MLM) is widely applied in both language pre-training and vision-language pre-training and has proven to be useful. For the input image-text token sequence, we randomly sample and mask 15% of tokens in the sequence while keeping the input image patch sequence untainted, similar to UNITER. The goal of masked language modeling task is to predict these masked tokens based on their surrounding context and visual information.

**Image-Text Matching.** Image-Text Matching (ITM) aims to determine whether the input image and text are matched or mismatched and is widely used in previous works. The model is given a batch of matched or mismatched image-text pairs, we apply a binary classifier on the concatenated of final representations of the cross-modal encoder to predict whether the image-text pair is matched or not.

## 4 Experiment

### 4.1 Implementation Details

Our pre-training data are composed of four existing image-text pairs datasets: COCO (Lin et al., 2014), Visual Genome (VG) (Krishna et al., 2017), Conceptual Captions (CC) (Sharma et al., 2018) and SBU Captions (Ordonez et al., 2011), which have also been widely used in previous VLP models and contain 4M images in total. We utilize CLIP-ViT-224/16 and RoBERTa-base to initialize the visual encoder and textual encoder of UNIMO-3. And the fusion encoder that consist of external cross-modal layer and internal cross-modal layer have a total of 6 layers, each with a hidden dimension of 768, intermediate size of feed-forward networks of 3, 072 and the number of heads of 12. The maximum length of the text sequence is set as 50. The image size is set to  $224 \times 224$  for pre-training. Same as previous works (Dou et al., 2022; Li et al., 2021), we apply RandAugment (Cubuk et al., 2020) for data augmentation and use the AdamW (Loshchilov and Hutter, 2017) optimizer with a base learning rate of  $1e-5$  and weight decay of 0.01. The learning rate is warmed up for 10% of the total training steps and then decayed linearly.

Following previous works, the learning rate of the cross-modal encoder is five times higher than that of uni-modal encoders. We pre-train UNIMO-3 for 100k steps on 8 NVIDIA A100 GPUs with a batch size of 4, 096.

We finetuning the UNIMO-3 model on the visual question answering (VQAv2) (Goyal et al., 2017), visual entailment (SNLI-VE) (Xie et al., 2019), and image-text retrieval (Flickr30K) (Young et al., 2014) tasks to evaluate the model’s performance. Following BridgeTower, we set image resolution as  $384 \times 384$  for these downstream tasks, except for VQAv2 as  $576 \times 576$ . And we also convert VQAv2 to a classification task with 3, 129 answer classes for fair comparison with previous works (Goyal et al., 2017; Teney et al., 2018).

### 4.2 Main Result

#### 4.2.1 Cross-modal Tasks

We compare UNIMO-3 to a variety of state-of-the-art models on cross-modal, visual and textual task. As shown in Table 1 and 2, we compare with a series of existing VLP models, including with only 4M images for pre-training models ViLT (Kim et al., 2021), UNITER (Chen et al., 2020), UNIMO (Li et al., 2020), UNIMO-2 (Li et al., 2022b), ALBEF (Li et al., 2021), VLMO (Bao et al., 2021), METER (Dou et al., 2022) and BridgeTower (Xu et al., 2022), and with a larger number images for pre-training models ALBEF, OFA (Wang et al., 2022), SimVLM (Wang et al., 2021) and BLIP (Li et al., 2022a). The base-size UNIMO-3 show competitive performances compared with the existing VLP models on downstream VL tasks. The best scores on each metric are marked in bold. UNIMO-3 achieves state-of-the-art performance on VQAv2 dataset, outperforming the previous SOTA model BridgeTower by 0.30% and 0.49% on test-dev and test-std. On the SNLI-VE dataset, UNIMO-3 demonstrate a stronger ability to determine the logical relationship between a natural language statement and an image. And on the Flickr30k dataset, UNIMO-3 also have impressive performance in recall metrics, outperforms even some larger-size models.

#### 4.2.2 Textual Tasks

To show the effectiveness of UNIMO-3 on textual tasks, we further compare with both VLP models including METER and BridgeTower, and pre-trained language model RoBERTa. The comparison results in Table 3 demonstrate that UNIMO-

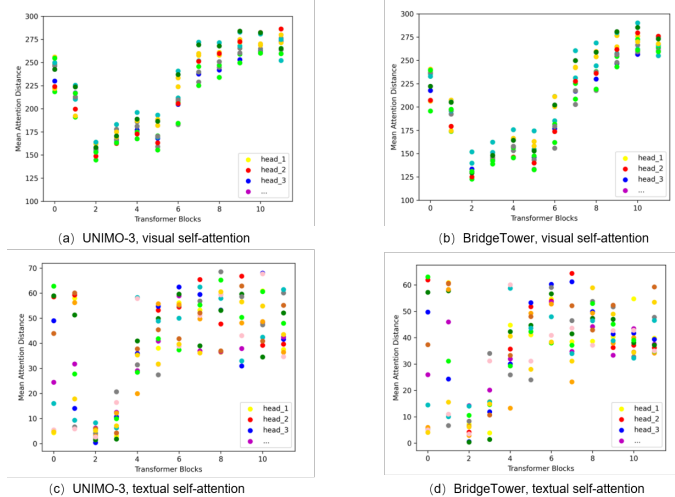


Figure 4: The average attention distance of BridgeTower and UNIMO-3.

Model	MNLI 392k	QQP 363k	QNLI 108k	SST-2 67k	CoLA 8.5k	STS-B 5.7k	MRPC 3.5k	RTE 2.5k	AVG
METER PT	87.25	89.09	92.72	94.65	61.14	90.65	92.12	79.06	85.84
BridgeTower PT	87.27	89.21	92.78	94.95	61.79	90.85	92.56	79.78	86.15 (+0.31)
UNIMO-3 PT	<b>87.28</b>	<b>89.09</b>	<b>92.69</b>	<b>94.86</b>	<b>62.82</b>	<b>90.19</b>	<b>92.81</b>	<b>80.52</b>	<b>86.28 (+0.44)</b>
RoBERTa-base	87.55	89.22	92.87	95.07	63.21	90.70	92.89	79.90	86.43

Table 3: Fine-tuning performance of text encoders (RoBERTa<sub>BASE</sub>) on GLUE dev sets before and after VLP. PT is short for Pre-Training. We report average scores and standard deviations over three runs of different random seeds. Matthews correlations are reported for CoLA, F1 scores are reported for QQP and MRPC, and Spearman correlations are reported for STS-B. The average of matched and mismatched accuracy scores are reported for MNLI.

3 achieves better performance than existing VLP models including METER and BridgeTower, and achieves comparable performance than existed PLMs such as RoBERTa on GLUE tasks. Especially, after vision language pre-training, on the RTE task UNIMO-3 textual encoder obtains 0.62 absolute gains compared to RoBERTa-base model.

### 4.2.3 Visual Tasks

For visual tasks, we evaluate UNIMO-3 on CIFAR-10 and CIFAR-100 datasets. Table 4 shows that, after vision language pre-training, the performance of our visual encoder drops most slightly on both tasks, achieves higher performance compared to METER and BridgeTower, average 0.43% accuracy improvement than METER. This further proves that the cross-layer and multi-granularity interaction mechanism adopted by the UNIMO-3 model can improve the fine-grained fusion of multimodal information while hardly affecting the effect of the visual encoder.

### 4.2.4 Scaling the Model

Despite the noteworthy results obtained by the UNIMO-3 model in a series of downstream VL tasks, we still expect the cross-layer interaction to show stronger performance on larger-scale models, thus we verified the performance of the scaled-up UNIMO-3-Large model. We replaced the UNIMO-3 uni-modal encoder with the corresponding large versions, we utilize CLIP-ViT-L/14 with 304M parameters for the visual encoder and RoBERTa-Large with 355M parameters for the textual encoder. For each layer of the cross-modal encoder, the hidden size was set to 1,024, the intermediate size of feed-forward networks was set to 4,096, and the number of heads was set to 16. Following the scaling-up version of BridgeTower, we set the patch size to 14x14, the image resolution to 294x294 during pre-training, and the image resolution to 574x574 during fine-tuning on VQAv2. As shown in Table 1, UNIMO-3-Large achieves 81.26 accuracy and 81.27 accuracy on the VQAv2 test-dev and test-std set.

Model	CIFAR-10	CIFAR-100	AVG
METER PT	98.46	89.52	93.99
BridgeTower PT	98.48	90.20	94.34 (+0.35)
UNIMO-3 PT	<b>98.55</b>	<b>90.30</b>	<b>94.42 (+0.43)</b>
CLIP-ViT-B-224/16	98.74	90.64	94.69

Table 4: Linear probe performance of CLIP-ViT-B-224/16 on CIFAR-10 and CIFAR-100 before and after VLP. PT is short for Pre-Training.



Figure 5: Visualization of the attention maps of BridgeTower and UNIMO-3 models. The example comes from the VQAv2 validation set. Predictions come from the fine-tuning checkpoints of both models.

### 4.3 Visualization

To demonstrate the effectiveness of the cross-layer multi-granularity interaction, we compare the pre-trained BridgeTower and UNIMO-3 models by analyzing the averaged attention distance (Xie et al., 2022) of different attention heads in both uni-modal layers and cross-modal layers. The average attention distance is a metric that measures how much other tokens each piece of tokens pays attention to. Similar to the receptive field in CNN that shows how much each pixel depends on other pixels. Different layers have different average attention distances, which indicates that they pay attention to different ranges of information. The higher the average attention distance, the more information each layer pay attention to, and vice versa.

As shown in Figure 5, we found that (a) In both the uni-modal encoder and cross-modal encoder, we observe a significant difference in average attention distance between different layers. Specifically, the average attention distance at the lower level varies widely across different heads, while it is relatively consistent in the upper level and tends

to be higher. This suggests that the cross-layer interaction we apply at higher layers focuses on more granularity information. (b) In contrast to the BridgeTower model, our model exhibits a higher value of the overall average attention distance. This implies that our model can focus on more granularity multimodal interaction at each layer and achieve more effective cross-modal alignment and fusion.

## 5 Conclusion

In this paper, we propose the UNIMO-3 model with stronger modeling ability for cross-modal fine-grained interaction. UNIMO-3 employs gating mechanisms to adaptively construct connections between each layer of the uni-modal encoder and each layer of the cross-modal encoder. Cross-layer interaction of different modal features enables effective interactive fusion of text and visual semantic information with different granularity. Sufficient experiments have proved that the UNIMO-3 model can achieve impressive performances in a series of downstream tasks.



## Ethics Statement

Our work complies with ACL Ethics, and all the codes and datasets used in our work comply with the ethics policy.

## References

- Stanislaw Antol, Aishwarya Agrawal, Jiasen Lu, Margaret Mitchell, Dhruv Batra, C Lawrence Zitnick, and Devi Parikh. 2015. Vqa: Visual question answering. In *Proceedings of the IEEE international conference on computer vision*, pages 2425–2433.
- Hangbo Bao, Wenhui Wang, Li Dong, Qiang Liu, Owais Khan Mohammed, Kriti Aggarwal, Subhojit Som, and Furu Wei. 2021. Vlmo: Unified vision-language pre-training with mixture-of-modality-experts. *arXiv preprint arXiv:2111.02358*.
- Yen-Chun Chen, Linjie Li, Licheng Yu, Ahmed El Kholy, Faisal Ahmed, Zhe Gan, Yu Cheng, and Jingjing Liu. 2020. Uniter: Universal image-text representation learning. In *Computer Vision–ECCV 2020: 16th European Conference, Glasgow, UK, August 23–28, 2020, Proceedings, Part XXX*, pages 104–120. Springer.
- Ekin D Cubuk, Barret Zoph, Jonathon Shlens, and Quoc V Le. 2020. Randaugment: Practical automated data augmentation with a reduced search space. In *Proceedings of the IEEE/CVF conference on computer vision and pattern recognition workshops*, pages 702–703.
- Alexey Dosovitskiy, Lucas Beyer, Alexander Kolesnikov, Dirk Weissenborn, Xiaohua Zhai, Thomas Unterthiner, Mostafa Dehghani, Matthias Minderer, Georg Heigold, Sylvain Gelly, et al. 2020. An image is worth 16x16 words: Transformers for image recognition at scale. *arXiv preprint arXiv:2010.11929*.
- Zi-Yi Dou, Yichong Xu, Zhe Gan, Jianfeng Wang, Shuohang Wang, Lijuan Wang, Chenguang Zhu, Pengchuan Zhang, Lu Yuan, Nanyun Peng, et al. 2022. An empirical study of training end-to-end vision-and-language transformers. In *Proceedings of the IEEE/CVF Conference on Computer Vision and Pattern Recognition*, pages 18166–18176.
- Yash Goyal, Tejas Khot, Douglas Summers-Stay, Dhruv Batra, and Devi Parikh. 2017. Making the v in vqa matter: Elevating the role of image understanding in visual question answering. In *Proceedings of the IEEE conference on computer vision and pattern recognition*, pages 6904–6913.
- Zhicheng Huang, Zhaoyang Zeng, Bei Liu, Dongmei Fu, and Jianlong Fu. 2020. Pixel-bert: Aligning image pixels with text by deep multi-modal transformers. *arXiv preprint arXiv:2004.00849*.
- Chao Jia, Yinfei Yang, Ye Xia, Yi-Ting Chen, Zarana Parekh, Hieu Pham, Quoc Le, Yun-Hsuan Sung, Zhen Li, and Tom Duerig. 2021. Scaling up visual and vision-language representation learning with noisy text supervision. In *International Conference on Machine Learning*, pages 4904–4916. PMLR.
- Wonjae Kim, Bokyung Son, and Ildoo Kim. 2021. Vilt: Vision-and-language transformer without convolution or region supervision. In *International Conference on Machine Learning*, pages 5583–5594. PMLR.
- Ranjay Krishna, Yuke Zhu, Oliver Groth, Justin Johnson, Kenji Hata, Joshua Kravitz, Stephanie Chen, Yannic Kalantidis, Li-Jia Li, David A Shamma, et al. 2017. Visual genome: Connecting language and vision using crowdsourced dense image annotations. *International journal of computer vision*, 123:32–73.
- Alex Krizhevsky, Geoffrey Hinton, et al. 2009. Learning multiple layers of features from tiny images.
- Junnan Li, Dongxu Li, Caiming Xiong, and Steven Hoi. 2022a. Blip: Bootstrapping language-image pre-training for unified vision-language understanding and generation. In *International Conference on Machine Learning*, pages 12888–12900. PMLR.
- Junnan Li, Ramprasaath Selvaraju, Akhilesh Gotmare, Shafiq Joty, Caiming Xiong, and Steven Chu Hong Hoi. 2021. Align before fuse: Vision and language representation learning with momentum distillation. *Advances in neural information processing systems*, 34:9694–9705.
- Wei Li, Can Gao, Guocheng Niu, Xinyan Xiao, Hao Liu, Jiachen Liu, Hua Wu, and Haifeng Wang. 2020. Unimo: Towards unified-modal understanding and generation via cross-modal contrastive learning. *arXiv preprint arXiv:2012.15409*.
- Wei Li, Can Gao, Guocheng Niu, Xinyan Xiao, Hao Liu, Jiachen Liu, Hua Wu, and Haifeng Wang. 2022b. Unimo-2: end-to-end unified vision-language grounded learning. *arXiv preprint arXiv:2203.09067*.
- Tsung-Yi Lin, Michael Maire, Serge Belongie, James Hays, Pietro Perona, Deva Ramanan, Piotr Dollár, and C Lawrence Zitnick. 2014. Microsoft coco: Common objects in context. In *European conference on computer vision*, pages 740–755. Springer.
- Ilya Loshchilov and Frank Hutter. 2017. Decoupled weight decay regularization. *arXiv preprint arXiv:1711.05101*.
- Vicente Ordonez, Girish Kulkarni, and Tamara Berg. 2011. Im2text: Describing images using 1 million captioned photographs. *Advances in neural information processing systems*, 24.
- Bryan A Plummer, Liwei Wang, Chris M Cervantes, Juan C Caicedo, Julia Hockenmaier, and Svetlana Lazebnik. 2015. Flickr30k entities: Collecting

- region-to-phrase correspondences for richer image-to-sentence models. In *Proceedings of the IEEE international conference on computer vision*, pages 2641–2649.
- Alec Radford, Jong Wook Kim, Chris Hallacy, Aditya Ramesh, Gabriel Goh, Sandhini Agarwal, Girish Sastry, Amanda Askell, Pamela Mishkin, Jack Clark, et al. 2021. Learning transferable visual models from natural language supervision. In *International conference on machine learning*, pages 8748–8763. PMLR.
- Shaoqing Ren, Kaiming He, Ross Girshick, and Jian Sun. 2015. Faster r-cnn: Towards real-time object detection with region proposal networks. *Advances in neural information processing systems*, 28.
- Piyush Sharma, Nan Ding, Sebastian Goodman, and Radu Soricut. 2018. Conceptual captions: A cleaned, hypernamed, image alt-text dataset for automatic image captioning. In *Proceedings of the 56th Annual Meeting of the Association for Computational Linguistics (Volume 1: Long Papers)*, pages 2556–2565.
- S. Shen, L. H. Li, H. Tan, M. Bansal, A. Rohrbach, K. W. Chang, Z. Yao, and K. Keutzer. 2021. How much can clip benefit vision-and-language tasks?
- Hao Tan and Mohit Bansal. 2019. Lxmert: Learning cross-modality encoder representations from transformers. *arXiv preprint arXiv:1908.07490*.
- Damien Teney, Peter Anderson, Xiaodong He, and Anton Van Den Hengel. 2018. Tips and tricks for visual question answering: Learnings from the 2017 challenge. In *Proceedings of the IEEE conference on computer vision and pattern recognition*, pages 4223–4232.
- Alex Wang, Amanpreet Singh, Julian Michael, Felix Hill, Omer Levy, and Samuel R Bowman. 2018. Glue: A multi-task benchmark and analysis platform for natural language understanding. *arXiv preprint arXiv:1804.07461*.
- Peng Wang, An Yang, Rui Men, Junyang Lin, Shuai Bai, Zhikang Li, Jianxin Ma, Chang Zhou, Jingren Zhou, and Hongxia Yang. 2022. Ofa: Unifying architectures, tasks, and modalities through a simple sequence-to-sequence learning framework. In *International Conference on Machine Learning*, pages 23318–23340. PMLR.
- Zirui Wang, Jiahui Yu, Adams Wei Yu, Zihang Dai, Yulia Tsvetkov, and Yuan Cao. 2021. Simvlm: Simple visual language model pretraining with weak supervision. *arXiv preprint arXiv:2108.10904*.
- Ning Xie, Farley Lai, Derek Doran, and Asim Kadav. 2019. Visual entailment: A novel task for fine-grained image understanding. *arXiv preprint arXiv:1901.06706*.
- Zhenda Xie, Zigang Geng, Jingcheng Hu, Zheng Zhang, Han Hu, and Yue Cao. 2022. Revealing the dark secrets of masked image modeling. *arXiv preprint arXiv:2205.13543*.
- Xiao Xu, Chenfei Wu, Shachar Rosenman, Vasudev Lal, and Nan Duan. 2022. Bridge-tower: Building bridges between encoders in vision-language representation learning. *arXiv preprint arXiv:2206.08657*.
- Peter Young, Alice Lai, Micah Hodosh, and Julia Hockenmaier. 2014. From image descriptions to visual denotations: New similarity metrics for semantic inference over event descriptions. *Transactions of the Association for Computational Linguistics*, 2:67–78.
- Yan Zeng, Xinsong Zhang, and Hang Li. 2021. Multi-grained vision language pre-training: Aligning texts with visual concepts. *arXiv preprint arXiv:2111.08276*.
- Pengchuan Zhang, Xiujun Li, Xiaowei Hu, Jianwei Yang, Lei Zhang, Lijuan Wang, Yejin Choi, and Jianfeng Gao. 2021. Vinvl: Revisiting visual representations in vision-language models. In *Proceedings of the IEEE/CVF Conference on Computer Vision and Pattern Recognition*, pages 5579–5588.